

THE X-RAY ABSORBER IN BROAD ABSORPTION LINE QUASARS

T. G. WANG,¹, W. BRINKMANN,² W. YUAN,³, J.X. WANG,¹ Y.Y. ZHOU¹*Draft version December 2, 2024*

ABSTRACT

Recent observations of Broad Absorption Line (BAL) quasars demonstrated that the soft X-ray emission of these objects is extremely weak and convincing evidence for very strong absorption by a high column density ($\sim 10^{23.5} \text{ cm}^{-2}$) was obtained for PG 1411+442, even though it is one of the few BAL QSOs strongly detected in soft X-rays. This paper examines the ionization status and geometry of the X-ray absorber by combining the properties of the UV lines with the X-ray continuum absorption. We show that the gas has to have large column densities in ions of major UV absorption lines, such as CIV, NV, OVI and Ne VIII, in order to have sufficient opacity around 0.2 to 0.35 keV. The UV absorption lines have to be saturated if the X-ray absorber intersects the line of sight to the UV continuum emission region. A uniformly covering UV and X-ray absorption model can be constructed for PG 1411+442 but in some other soft X-ray detected BAL QSOs, such as PG 1001+054, the observed line optical depth is much lower than expected from the X-ray absorbing material. We propose a scheme in which a substantial fraction of the line of sight to the continuum source may be covered by either an optically thick flow or clouds in a narrow velocity range, but in which the total covering factor of either the whole flow or all clouds is close to unity.

The absorber can contribute significantly to the extremely highly ionized emission lines, such as O VI 1032/1037Å and Ne VIII 770/780Å if it covers a substantial fraction of solid angle and if the density is higher than 10^8 cm^{-3} . However, it has very little impact on the medium and low ionization UV lines such as NV, CIV. The profiles of NeVIII and OVI lines may be indicators for the kinematics of the X-ray absorber in QSOs. The observed Ne VIII line profiles in QSOs suggests that the velocity of the gas projected onto our line of sight is similar to that seen in the outflows of the UV BALs.

1. INTRODUCTION

Broad Absorption Lines (BALs) are prominent features in the UV spectra of $\sim 10\text{--}15\%$ of optically selected quasars. The lines are formed in ionized winds in which the speeds can range from near zero to more than 30,000 km s^{-1} . The absorption features most commonly observed are Ly α $\lambda 1216$, CIV $\lambda 1549$, SiIV $\lambda 1397$, and NV $\lambda 1240$. Low ionization broad absorption lines (LoBALs), such as MgII $\lambda 2798$ and Al III $\lambda 1857$ are detected in about 15% of the objects. For two BAL QSOs, higher ionization lines, up through Ne VIII $\lambda 774$, Mg X $\lambda 615$, Si XII $\lambda 499$, are reported from UV observations with HST and HUT (Korista & Arav 1997, Telfer et al. 1998). Since most BAL QSOs are only observed by ground based optical telescopes which can not access the spectral range of these very high ionization lines, the true incidence of the very high ionization BALs is not known.

The observed frequency of BALQSOs among all quasars, combined with the assertion that the absorbing material covers ≤ 0.2 of the solid angle, leads to the conclusion that every QSO has outflows which intercept only a fraction of the solid angle of the central object (e.g., Hamann, Korista & Morris 1993). This picture is supported by the similarity of UV continuum and emission line properties of BAL and non-BAL QSOs (Weymann et al., 1991). The BAL region covers, at least partially, the broad emission line region since the NV absorption trough is usually deeper

than the local continuum. The large momentum of radiation absorbed by resonance transitions is probably responsible for the acceleration of the gas. The signature of a kick-off effect at velocities of about 6000 km s^{-1} further supports this picture (Arav, Li & Begelman 1994).

Establishing the physical properties of the flow is a fundamental issue in BAL studies. Earlier work was solely based on a few prominent UV absorption lines, usually CIV, Ly α , NV, SiIV, and, for LoBAL, MgII and AlIII, with the assumption that the absorbing material fully covers the emission region and is not seriously saturated. These studies suggested an over-abundance of metals; C and N are, relative to H, enhanced by a factor 3-5 and an even larger abundance for Si was deduced. More recently, based on the detection of P V absorption lines, Haman (1998) argued for a large column density instead of extremely high phosphorus abundance. From the UV spectra taken by the Hubble Space Telescope of high or moderate redshift BAL QSOs, the line profiles of many more lines, including lines from different ionization stages of the same element, were measured for several objects. These observations indicate that either the absorbing material only covers partially the line of sight to the continuum or the scattered light fills in the absorption trough (e.g., Arav et al. 1999). The fact that the spectro-polarimetry of BAL usually shows higher polarization in the BAL trough than for the continuum and emission line region also favors the

¹Center for Astrophysics, University of Science and Technology of China, Anhui, 230026, CHINA (email:twang@ustc.edu.cn)²Max-Planck-Institut für extraterrestrische Physik, Giessenbachstrasse, D-85740 Garching, FRG³Space Astrophysics Group, National Space Development Agency of Japan (NASDA), Tsukuba Space Center, Sengen-2-1-1, Tsukuba, Ibaraki 305 JAPAN

latter interpretation (e.g., Schmidt & Hines 1999, and references therein).

X-ray spectra, even at their currently relatively low resolution, have the advantage that photo-electric X-ray absorption does not have saturation problems and that it can be used to measure the total absorption column density. As a result, the light from the scattering medium or the leakage of a partially covered absorber is distinguishable from the transmitted light, thus allowing measurement of the effective covering factor of the absorber.

BAL QSOs had not been targets for a systematic study in the X-ray band until their extra-ordinary properties in the soft X-ray band were discovered by ROSAT (Green et al. 1995, Green & Mathur 1996), and they remain a rare class with extremely weak X-ray emission. In the soft X-ray band, there are only four reported cases of detections (PG 1411+442, PG 1001+054, PG 2112+059, SBS 1542+541 (Brinkmann et al. 1999, Brandt et al. 1999, Telfer et al. 1998) showing apparent broad band optical-to-X-ray spectral indices $1.85 \leq \alpha_{ox} \leq 2.25$, while only upper limits are available for the other objects. ROSAT observations of the LoBAL QSO PG 1700+518 yield an even higher upper limit of $\alpha_{ox} > 2.3$ (Wang et al. 1996), and the current X-ray observations are not sensitive enough to establish how high these values really are. However, we noticed that a ROSAT detection is more likely for weak BAL objects. Two ROSAT detections, Mrk 231 and IRAS 07598+6508 (marginal), are probably associated with the circumnuclear starburst instead of nuclear activity (Turner 1999). The weak X-ray emission was interpreted to be due to strong absorption, instead of an intrinsically X-ray weakness of the sources. This required a column densities of $10^{23-24} \text{ cm}^{-2}$ (Brinkmann et al. 1999, Wang et al. 1999, Gallagher et al. 1999).

Therefore, a critical question arises whether the UV and X-ray absorber is the same material. What is the geometry of this absorber? What is the ionization status? In this paper, we try to address these questions by examining the ionization status of the X-ray absorber in the BAL.

2. IONIZING CONTINUUM

The shape of the ionizing continuum is crucial for the determination of the ionization structure of the photo-ionized gas. For non-BAL QSOs, an average spectrum is derived by combining the soft X-ray spectrum at the low redshift end and the HST far-UV spectrum at high redshifts (Laor et al. 1997, Zheng et al. 1998). However, we cannot construct a mean ionizing continuum for BAL QSOs in this way as soft X-ray emission has not been detected from most BAL QSOs. In addition, it is believed that the few detections do not show the intrinsic spectrum but only the scattered/leaked component of the primary emission. The only reported detection of the primary X-ray component is PG 1411+442 in the medium energy X-ray band by ASCA.

The simultaneous analysis of the ROSAT and ASCA data of PG 1411+442 was presented by Brinkmann et al. (1999); a more extended treatment combining the UV data from HST and the X-ray data from ROSAT and ASCA can be found in Wang et al. (1999). They found a primary X-ray component absorbed by $2.5 \times 10^{23} \text{ cm}^{-2}$ and scattered flux at about 3-5 per cent of the intrinsic emission. It is worthwhile to point out that although they assumed

the photon index of high energy component (Γ_{high}) to be 2.0 because it ($2.2^{+0.8}_{-0.7}$ for 2.7σ error bar) was not well constrained by the fit, the absorption is well constrained to be larger than $1.5 \times 10^{23} \text{ cm}^{-2}$ (at 90% confidence level) even when the Γ_{high} is left as a free parameter.

Figure 1 shows the Spectral Energy Distribution (SED) of PG 1411+442 from the optical to the X-ray band. The infrared to optical data have been taken from Neugebauer et al. (1987). The UV spectrum from IUE between 2000-3000Å is extracted from the IUE final archive and corrected for the Galactic reddening $E(B-V)=0.03$ ($N_H^G=1.4 \times 10^{20} \text{ cm}^{-2}$). Reddening corrected HST spectra were taken from Wang et al. (1999). In the X-ray band, the observed ROSAT and ASCA spectra are shown (model A of Wang et al. 1999). A composite radio-quiet QSO spectrum from the optical to the X-ray band obtained by combining the results from Zheng et al. (1998) and Laor et al. (1997) is plotted for comparison. The absorption corrected infrared to X-ray spectrum of PG 1411+442 is clearly similar to that of average radio-quiet quasars. For the above broken power-law model with absorption as a free parameter, the intrinsic 1350Å to 1 keV spectral index is $1.55^{+0.20}_{-0.33}$ (only taking into account the X-ray flux uncertainty).

Figure 1 also shows the SED of two other BAL QSOs, PG 1001+054 and PG 2112+059, detected by ROSAT. The ROSAT spectra were fitted with an absorbed power law. Absorption ($N_H = 2.8^{+6.3}_{-2.4} \times 10^{20} \text{ cm}^{-2}$) in excess of the Galactic one is not needed for PG 1001+054; therefore, the column density is fixed at the Galactic value ($1.9 \times 10^{20} \text{ cm}^{-2}$), and the fit yields a photon index $\Gamma = 3.5^{+0.6}_{-0.4}$. However, the X-ray flux at 1 keV is lower by a factor of 50 compared to the mean radio-quiet QSOs. This is unlikely to be intrinsic since the HeII $\lambda 1640$ is fairly strong in the HST spectrum (Fig. 2) of PG 1001+442 with an equivalent width larger than that in the composite HST QSO spectrum (Zheng et al. 1998), implying that the ionizing continuum seen by the BLR should be hard (Korista, Ferland & Baldwin 1997). The strength of CIV line, found to correlate with ionizing continuum spectral index (e.g., Wang et al. 1998), also indicates hard continuum spectrum. In fact, the apparent broad band spectra of PG 1001+059 and PG 1411+442 from the infrared to soft X-rays are similar. Therefore, we believe that the ROSAT spectrum is also the scattered component, as in PG 1411+442, and that the fraction of scattering is even lower in this object. The interpretation of scattering is consistent with the fact that the ROSAT spectral index of PG 1001+054 fits well to the FWHM of H β versus spectral index correlation (see Wang, Brinkmann, & Bergeron 1996, Laor et al. 1997).

The situation for PG 2112+043 is slightly more complicated. Large absorption is certainly present. By fixing the photon index to the average value of 2.7 of the radio-quiet PG quasars a power law fit with free absorption yields an optical to X-ray spectral index 2.0 ± 0.2 and an absorption column density $N_H = 7^{+8}_{-4} \times 10^{21} \text{ cm}^{-2}$, where errors are given at 90% confidence levels for one parameter. Clearly, the absorption corrected flux is still lower by a factor of about 5-10 with respect to that of average QSOs (see also Figure 1). It is, however, not clear whether the ROSAT spectrum represents the transmitted continuum or a combination of scattered plus transmitted component. Complicated ab-

sorption models such as a partially covered high column plus a uniformly covering low column absorber can reproduce the feature as well.

In summary, so far it appears that the observed broad SEDs of BAL QSOs are consistent with the intrinsic SED of typical non-BAL QSOs modified by absorption in the soft X-ray band. For this reason, we will use the average quasar spectral energy distribution in our calculations. However, there is no guarantee that it represents the typical SED of BAL QSOs, since the ROSAT detected BAL QSOs only account for a small fraction of all BAL QSOs and there are some indications that they are special; for example, the strength of the CIV BAL in these objects is lower than the average value for BAL QSOs (Weymann et al. 1991).

3. PHYSICAL PARAMETERS: GENERAL CONSIDERATIONS

In this section, we summarize the ranges of the physical parameters, obtained either directly or estimated from observations. For the estimates derived from the UV spectrum, we assume that the X-ray absorber fully covers the UV continuum source.

Column density: The column density for PG 1411+442 has been determined to be $N_H = 2.5 \cdot 10^{23} \text{ cm}^{-2}$. Although the column densities for other BAL QSOs have not directly been measured, they are likely similar or even larger. The fact that the X-ray emission from BAL QSOs is very weak, even in the ASCA band, constrains the column densities to be higher than a few times 10^{23} cm^{-2} in most bright BAL QSOs if their intrinsic X-ray emission is comparable to that of the other radio-quiet QSOs (Brinkmann et al. 1999, Gallagher et al. 1999). Thus, a typical column density of $10^{23.5} \text{ cm}^{-2}$ seems to be a quite conservative estimate.

Density: The density of the absorbing gas is virtually unknown. However, for a photo-ionized gas the ionization structure is not sensitive to the density. The lack of broad [OIII] emission in QSOs suggests that the typical density of an UV absorber is higher than 10^8 cm^{-3} . This conclusion, however, is somewhat ionization-dependent. If the BAL region is highly stratified and Oxygen is ionized beyond [OIII] as our calculations for X-ray absorber show (see sect. 4.1), then there are no constraints for a lower limit to the gas density in the highly ionized zone. Earlier reports of a possible detection of absorption lines from excited ions OV* and CIII* (Pettini & Boksenberg 1986, Korista et al. 1992) require an even higher density ($n_e \simeq 10^{11} \text{ cm}^{-3}$). These results were questioned by later high S/N observation (Arav et al. 1999). A rather large range of densities might co-exist in the BAL region and Arav et al. proposed dense flow tubes embedded in a low density global flow to explain the ionization dependent covering factor.

Metal abundances: BAL quasars are claimed to have remarkably high abundances of heavy elements relative to the solar values. C, Si, N, P, and Fe are over-abundant by 1-2 orders of magnitude. The abundances were derived from the optical BAL depths together with photoionization models assuming ionization equilibrium. The enhancement of metal elements can be reduced, but not eliminated, by using complicated shapes for the ionizing continuum. The qualitative results will not be altered by considering saturation of the absorption lines since troughs

in CIV and NV are much deeper than in Ly α . The calculations presented below, however, are based on cosmic abundances, since little is known about the abundances of the X-ray absorber, which might be different from that of the UV absorbing gas. Since the X-ray opacity is mainly determined by heavy elements, the column density mentioned above actually measures that of the heavy elements; therefore, the results are correct as far as the metals are concerned. The hydrogen column density is roughly inversely proportional to the measured metal abundance. The reason is that for lower abundances thicker material is needed to produce the same X-ray absorption, and the X-ray column density is the equivalent hydrogen density with solar metal abundances.

Ionization parameter: An upper limit on the ionization parameter for the X-ray absorber can be obtained by requiring that the material is not too highly ionized to be transparent for the low energy soft X-rays. Brinkmann et al. (1999) showed that a uniformly covering warm absorption model does not fit the ROSAT+ASCA spectra of PG 1411+442, and they argued for a partially covering absorption model or for an absorption plus scattering model. However, both Brinkmann et al. and Wang et al. simply used a neutral absorber. We show below that combining the ROSAT and ASCA spectrum can put a tight upper limit on the ionization parameter of the absorber.

Allowing the absorbing medium to be partially ionized, we use the ionized absorption model *absori* in XSPEC to replace *wabs* for the model of an absorbed, broken power law plus a scattering component by electrons (see Wang et al. 1999 for details). The break energy has been fixed at 1.0 keV and the photon index of the hard X-rays at $\Gamma=2.0$. The ionizing continuum is assumed to be a power law with a photon index 2.5 from the UV to hard X-rays. This simplified continuum is not an exact representation for the ionizing continuum but it produces similar results as Netzer's more complicated model for PG 1126-041 (H. Netzer, private communication). We use an X-ray ionization parameter U_x , which is defined as the dimensionless ratio of photon density above 0.1 keV and the particle density (Netzer 1996), instead of $\xi = L/(nr^2)$, since it is much less dependent on the detailed UV to X-ray spectral slope. Figure 3 shows 68%, 90% and 99% contours for the ionization parameter versus the column density for the absorbing material. The upper limit on U_x is mainly constrained by the photon flux at energies lower than 0.4 keV, and depends only weakly on the column density. At $N_H = 2 \cdot 10^{23} \text{ cm}^{-2}$, one obtains $U_x < 0.11$ (at 90% confidence level, see Fig. 3). For the SED of average radio-quiet quasars, linearly extrapolated from the UV to X-ray energies, the hydrogen ionization parameter is $U_H = 35 U_x$.

If we assume that the intrinsic X-ray spectrum of PG 1001+054 is similar to an average radio-quiet QSO, the unabsorbed X-ray flux will be by a factor 30 greater. We fitted the ROSAT spectrum with a two component model, in which a primary power law continuum, 30 times larger than the observed one, is completely covered by an ionized absorber and an electron-scattered continuum component which is only absorbed by the Galactic absorption, similar to the model for PG 1411+442. Taking typical column density ($N_H = 10^{23.5} \text{ cm}^{-2}$) for the ionizing material, an upper limit (at 90% confidence level) of $U_x < 0.2$ can be estimated. The exact value is dependent on the assumed

column density as well as assumption of the intrinsic continuum.

A lower limit on the ionization parameter can be obtained by considering the absorption by hydrogen. In the HII zone, the fraction of neutral hydrogen is approximately $n(H^0)/n(H^+) \simeq 10^{-5.3}/U_H$ for a gas photo-ionized by a typical AGN continuum (Netzer et al. 1990). The ratio would be lower than that given above when the ionization parameter is high, so that collisional ionization becomes significant. Since the Lyman break is not severe for most HI BAL QSOs (Korista et al. 1992, Arav et al. 1999) this puts an upper limit on the total column density of neutral hydrogen on the line of sight to the UV continuum emission region to be less than $10^{17.3} \text{ cm}^{-2}$ ($\tau_{912} \simeq 1$). For typical column densities this implies a lower limit of $U_H = 5$ if the X-ray absorber fully covers the UV continuum emission region. A tighter constraint on the neutral hydrogen column density can be derived by using the Ly α line absorption but required a knowledge of the distribution of HI column density in velocity space.

4. PREDICTED ABSORPTION AND EMISSION LINES

4.1. *Absorption Lines*

In order to qualitatively estimate the ionization status of the heavy elements, we first consider the source of opacity in the 0.2 to 0.4 keV soft X-ray band. For a weakly ionized gas helium is a major contributor to the opacity. However, if the hydrogen Lyman break is not severe, helium atoms will produce negligible absorption in 0.2-0.4 keV band. The fraction of He^+ can be roughly estimated from $He^{++}/He^+ \simeq 10^{3.2}U_H$ for the typical ionizing AGN continuum (Netzer et al. 1990). This gives $H^0/He^+ \simeq 0.1$ for gas dominated by He^{++} . Since the photo-electric absorption cross section decreases with photon energy as E^{-3} , in order to produce an optical depth of order $\tau = 1$ at 0.2 keV, an optical depth $\tau(54\text{eV}) \simeq 51$ is required! This implies an optical depth at the Lyman limit of the order of 9. Therefore it appears unlikely that helium contributes significantly to the opacity at 0.2 keV without producing a serious Lyman break. Thus the 0.2 to 0.4 keV opacity must be produced by heavy elements.

Figure 3 shows the ionization potentials (IPs) of the valence electrons for the ions of the four most abundant elements C, O, N, and Ne. The IPs for the first K-shell electrons are 392, 552, 739 and 1196 eV for C, N, O and Ne, respectively. From this plot, it is clear that, in order to have a significant opacity below 0.35 keV, a substantial fraction of the elements O and Ne must keep at least one L-shell electron, i.e., they are not ionized beyond O^{5+} and Ne^{7+} . Note that O^{5+} and Ne^{7+} are also ions which produce major resonant UV absorption lines. The fact that resonant line absorption has a much larger cross section than photo-electric absorption (by a factor of order 10^4) suggests that the optical depth of the line absorption is much larger than the absorption edge in the soft X-ray band if OVI and NeVIII are responsible for the X-ray absorption. The large absorption in the soft X-rays at energies as low as 0.3 keV requires that OVI and NeVIII absorption lines in the X-ray absorbing gas must be optically very thick. This general result is not strongly dependent on the specific SED or on the relative metal abundances of O and Ne. A detailed ionization calculation (see below)

shows that in photo-ionization equilibrium a substantial fraction of CIV and NV should also exist in this case.

For the calculations a plane-parallel geometry is adopted and the ionizing continuum for average radio-quiet quasars illuminates one side. A typical column density of $10^{23.5} \text{ cm}^{-2}$ is assumed. The ionization equilibrium is determined by using the photoionization code CLOUDY 94.01 (Ferland 1999). Figure 4 shows the ionization structure of the elements carbon, nitrogen, oxygen and neon for an ionization parameters $U_H=10$. In this plot, C^{3+} , N^{4+} , O^{5+} , Ne^{6+} , and Ne^{7+} coexist over a very large region. The opacity at energies between 0.1keV and 0.35 keV are mainly due to the ions O^{5+} , Ne^{7+} and Ne^{6+} .

The transmitted continua are plotted in Fig. 5 for $U_H = 8, 10$, and 16 . A substantial Lyman edge is seen only in the first case, but a substantial HeII edge at 54.4 eV is present in all cases. This is because in a gas ionized by a typical AGN-continuum, $He^{++}/He^+ \simeq 10^{3.2}U_H$. This means that the column density of He^+ is larger than that of H^0 by a factor of nearly 10 in a fully ionized gas. It can be seen that only when $U_H \leq 10$ for the given column density, a large fraction of the soft X-rays between 0.2-0.3 keV can be absorbed. This corresponds to $U_X \simeq 0.29$, which is roughly consistent with that derived from the X-ray spectral fits for PG 1411+442. The soft X-ray opacity between 0.1 to 0.3 keV is mainly caused by OVI, NeVII, and NeVIII ions, whose abundances are very sensitive to U_H , as can be seen in the figure.

Table 1 shows the predicted column densities for $U_H = 10$ and $U_H = 8$. As one can see from the table, the absorber can certainly predict a large column density in ions producing the major UV absorption lines within the allowed range of ionization parameters. At $U_H=10$, the model predicts CIV and NV column densities close to the total column densities estimated from strong BALs, and an OVI column density much larger than previously estimated based on the UV absorption line. An even larger column density is produced for NeVIII lines. Further, the column density of neutral hydrogen is an order of magnitude higher than required by Ly α absorption. Since the column densities of these ions of CIV, NV, OVI and NeVII increase rapidly with decreasing ionization parameters and $U_H = 10$ is an upper limit imposed by requiring strong absorption in the 0.2-0.35 keV band, the above column densities represent only lower limits.

Since both, Ly α absorption and the Lyman edge, are sensitive to the exact value of the ionization parameter and the metal abundances, the lower limit for the ionization parameter can be dramatically relaxed for much higher metal abundances or a very steep ionizing continuum. Since the fraction of neutral hydrogen is only proportional to U_H^{-1} , the reduction of the fraction of hydrogen by an order of magnitude, while keeping the X-ray opacity constant would require the ratio U_H to U_x to be ten times larger, implying a very steep UV to X-ray spectrum $\alpha_{uvx} \simeq 2.3$. This seems very unlikely in view of the results of 1411+442, where 1350\AA to 1 keV spectral index $\alpha_{uvx} = 1.55^{+0.20}_{-0.33}$ when corrected for the intrinsic absorption (see section 2). If the metal abundances are one order of magnitude higher, the hydrogen column can be lower by a similar factor, because the absorption in the X-ray band is mainly due to metal elements.

In order to see how the predicted column densities

change with the assumed hydrogen column density, we calculated similar models for $N_H = 10^{22.5}$ and 10^{23} cm^{-2} . The density and ionizing continuum were the same as used in the previous calculations. In order to limit the transmitted 0.2-0.3 keV flux to less than 30% of the primary, the ionization parameters (U_H) had to be less than 1.4 and 3.6 for $N_H = 10^{22.5}$ and 10^{23} cm^{-2} , respectively. For these U_H 's, the predicted column densities of C^{3+} , N^{4+} , O^{5+} , Ne^{6+} , and Ne^{7+} are similar to those of the $N_H = 10^{23.5} \text{ cm}^{-2}$ case (see Table 1), as expected. We did not calculate the column density for the $N_H = 10^{24} \text{ cm}^{-2}$ model since the escape probability approximation used in Cloudy may result in an incorrect ionization structure (Dumont, Abrassart & Collin 2000). But the argument presented at the beginning of this section suggests that the ion column densities should be similar.

Although our calculations are only carried out for a one-component model, more complicated models, such as multiple-zone models, should produce strong CIV, NV, OVI absorption lines as well. In order to isolate the zone which produces the absorption lines, we considered a two-zone model. The X-rays at energies at >0.35 keV are absorbed by a high column, highly ionized absorber, in which the C, N, O atoms are ionized beyond CIV, NV, OVI, and at lower energies by a low column density, low ionization material. Since the high ionization zone contributes little to the X-ray absorption below 0.35 keV, the opacity below 0.35 keV has to be dominated by the low ionization material. The main contribution to the opacity between 0.2-0.4 keV is from N, O, and Ne at moderately high ionization parameters, and from He at low ionization parameters, when He^+ is the dominating species. In the former case, an argument similar to the one given at the beginning of this section suggests large absorbing column densities in CIV, NV, OVI, NeVII and NeVIII. In the latter case, a large optical depth at the Lyman limit is predicted, and strong absorption by lines from low ionization species such as OIII, CIII, NIV, etc. seems inevitable.

4.2. Emission Lines

Absorption lines can only trace the outflowing material along the line of sight, while information on the global distribution of the gas has to be deduced by other means. Emission lines represent one such tool.

From the ionization structures given by the above calculations it is clear that the X-ray absorbing gas cannot contribute much to the emission lines from low ionization species. The line emission, unlike the ionization structure, depends critically on the particle density as well as on the EUV and soft X-ray spectral slope. For a density of 10^9 cm^{-3} and $U_H = 10$, the model predicts EWs of 31Å for OVI $\lambda 1032\text{\AA}$ and 21Å for the NeVIII $\lambda 770/780\text{\AA}$ emission line, for a covering factor of 1.0. These values are a factor of two and three higher than the average EWs for these lines measured by HST (Hamann et al. 1998). The line EWs increase to 77Å for OVI and 39Å for Ne VIII for $U_H = 8$. The absorber can make a significant contribution to the emission of NeVIII and OVI unless it covers only a small fraction of the solid angle or the density of the gas is small. In fact, Hamann et al. (1998) discussed already the possibility of NeVIII emitting gas associated with the warm absorber in the X-ray band. Hamann et al. (1998) found that the NeVIII lines are significantly broader than

CIV in PKS 0355-483 and PG 1522+101. From their figures, the line widths extend over the velocity range seen in typical BAL QSOs.

5. COMPARISON WITH OBSERVATIONS

PG 1411+442: Since the residual fluxes in the CIV and NV absorption troughs are similar to the fraction of the unabsorbed X-ray flux, Wang et al. (1999) argued that they are severely saturated at the bottom, but the observed residuals are the leaked light. This makes any estimate of the total column densities of CIV and NV very difficult and only lower limits can be derived. The minimum column densities required to reproduce the observed CIV and NV absorption features are of the order of 10^{16} cm^{-2} for C^{3+} and N^{4+} , and thus, are consistent with the expected lower limits to the column densities of these ions from the X-ray absorber estimated in section 4. The SiIV absorption line appears not to be saturated in this object; a column density of $2 \cdot 10^{14} \text{ cm}^{-2}$ ($\text{EW} \simeq 6\text{\AA}$) is derived. Substantial SiIV can be present only in the zone where the carbon is dominated by CIV or lower stages. The ionization parameter ($U_H \simeq 5$) is lower than the upper limit set by the soft X-ray absorption in the last section in order to reproduce the SiIV absorption line for the column of $2 \cdot 10^{23} \text{ cm}^{-2}$ derived from the X-ray absorption. This results in a higher column density ($10^{16-17} \text{ cm}^{-2}$) of HI for cosmic abundances, and higher CIV and NV column densities. The box-shaped profile with substantial residual flux in the $\text{Ly}\alpha$ absorption line trough suggest that the absorption line is saturated, but the covering factor is smaller than 1 (~ 0.8). Thus, the observed HI column density can be consistent with the expectation from the X-ray absorber. The lower covering factor (0.8) may be due to the partially covering of the broad emission line region by the absorbing gas as part of Lyman emission line may be produced in a region more extended than CIV emission region. Thus, in PG 1411+442, the observed UV and X-ray data are consistent with a uniformly covered absorber model. Notice that the situation should be similar for other BAL QSOs with saturated absorption line troughs.

PG 1001+054: If the intrinsic broad band spectrum of this object is similar to other radio quiet AGN, i.e., $\alpha_{ox} = 1.65$, the detected soft X-ray component can not be the transmitted one as it is rather steep. Most likely, we have a similar scenario as in PG 1411+442. The fraction of scattering is comparable, a few percent. Since the residual flux in the CIV absorption line in this object is more than 30% of the continuum, even at the deepest part of the trough, the observed profile implies either that the optically thick absorbing material is leaky and covers less than 70% of the sky or that the gas is not optically thick to the continuum photons. With the latter assumption, the total column density in CIV ions is estimated to be $\simeq 2 \cdot 10^{15} \text{ cm}^{-2}$ ($\text{EW} \simeq 13\text{\AA}$). Since the ROSAT spectrum is very steep, no leaking component is seen, not even in the hard band of the ROSAT PSPC, and therefore an absorption column density of at least a few times 10^{22} cm^{-2} is required for X-ray absorber. Similarly, to keep sufficient opacity in the low energy soft X-ray band requires that a substantial fraction of O and Ne atoms must be at ionization stages equal to or lower than OVI and NeVIII. If the continuum is not too different from the average quasar

TABLE 1
PREDICTED COLUMN DENSITIES FOR DIFFERENT BAL IONS

$\log N_H$	23.5		23	22.5
U_H	10	8	3.6 ^a	1.4 ^a
CIV	2.4×10^{16}	8×10^{16}	3.2×10^{16}	2.8×10^{16}
NV	3.4×10^{16}	9×10^{16}	4.7×10^{16}	4.8×10^{16}
OVI	1.2×10^{18}	4×10^{18}	1.8×10^{18}	1.9×10^{18}
NeVII	5.2×10^{17}	4×10^{18}	7.4×10^{17}	7.5×10^{17}
NeVIII	3.7×10^{18}	6×10^{18}	2.3×10^{18}	1.4×10^{18}
HI	3.0×10^{16}	4×10^{16}	3.4×10^{16}	4.0×10^{16}

^aThe photo-ionization parameters for a single zone constrained to transmit about 30% of the intrinsic 0.2-0.3 keV soft X-ray flux.

SED, the X-ray absorber would produce column densities of a few 10^{16} cm $^{-2}$ for CIV and NV (see table 1). This number is much larger than that inferred from the UV absorption lines. The discrepancy can hardly be explained by source variability as one needs a factor of 10 brighter X-ray emission in order to match 30% residuals in the absorption line trough, considering the fact that statistically no BAL QSOs show strong X-ray emission. Although we cannot rule out that an agreement can be achieved by using a completely different ionizing continuum, that of Mathews & Ferland (1987) with a bump in the EUV still predicts a column density in CIV $> 10^{16}$ cm $^{-2}$ if the transmitted flux between 0.2-0.3 keV is less than 30%. For a power law spectrum for the EUV (from 13.6 eV to 0.2 keV) ionizing continuum, the spectral index α ($f_\nu \propto \nu^{-\alpha}$) is required to be larger than 2.2 in order to match the observed CIV column density. This seems unlikely in view of our discussion presented in section 2.

Therefore, we prefer a picture in which an optically thick absorber partially covers the UV continuum source. There are two different type pictures for the partial covering. In the first case, the X-ray absorbing material only partially covers the UV continuum emission region, but fully covers the X-ray continuum region. This means that the UV emission region is significantly larger than the X-ray emission region. However, it requires that the absorbing material is close to the central source. This seems unlikely as the NV absorption line profile indicates that the BAL gas is located at a distance at least as large as the emission line region.

An alternative picture is that the line absorption at a given velocity is saturated but the absorbing material at the velocity only partially covers the line of sight to the continuum source, resulting in an apparently low column density in the absorption line. In order to explain the nearly complete absorption in the soft X-ray band, we require that the global covering factor of the absorber, via integrating the covering factor at different velocities, is equal or very close to unity. This can be realized by allowing the material at different velocities to intersect the line of sight to different parts of the continuum. The partial covering

at a given velocity is either due a patchy absorber with covering factor of less than one or due to continuous outflow with cross section smaller than the continuum source. One consequence of this kind of model is that the covering factor at any specific velocity is dependent on the angle between the line of sight and the iso-velocity surface. In the clouds model, larger viewing angle produces larger covering factor since more clouds on the iso-velocity surface enter the line sight to the continuum source. The opposite behavior is predicted for the small cross-section outflow model since the covering factor at a specific velocity in this case is the projected area of the iso-velocity surface onto the line of sight to the UV continuum divided by the area of the UV emission region, which decreases with the viewing angle. With this picture, the different covering factor of PG 1411+442 and PG 1001+054 might be just due to an aspect effect, instead of intrinsically different covering factor of this absorber. Future X-ray observation of the photo-electric iron K edges should be able to reveal such velocity dependent partially covering features.

It is worthwhile to point out that the situation for the ROSAT undetected low redshift bright QSOs with shallow BAL troughs is similar to that of PG 1001+054. However, this is hard to confirm for high redshift BAL QSOs because the 0.2-0.35 keV band is shifted out of the ROSAT windows. Due to strong Galactic absorption below 0.1 keV, future missions more sensitive at soft X-rays might also have difficulties to settle this question for the BAL QSOs beyond redshifts of 1.5.

SBS 1542+541: This is one of the highly ionized UV absorption line BAL QSO. The CIV and NV absorption lines are weak, but absorption lines from OVI or higher ionization stage ions are strong. The optical to X-ray spectral slope was found to be $\alpha_{ox} = 1.86$ using ROSAT data (Telfer et al. 1998), which is significantly smaller than the value found for other BAL QSOs. The S/N ratio of the ROSAT data is too low to allow detailed spectral fits. Since the ionization of BAL gas is much higher than conventionally observed in other BAL QSOs, it is likely that the ionization parameter is also higher in this object, and thus, it appears possible that a directly transmitted con-

tinuum is detected by ROSAT. Given the redshift of $z = 2.361$ for this object, ROSAT actually measured the continuum in the 0.4-8.0 keV band in the rest frame of the QSO. The transmission of X-rays at medium energies is not very sensitive to the exact value of the ionization parameter and is only a function of the total column density, provided that the ionization parameter is not too high. Telfer et al. (1998) proposed an ionization dependent covering factor model to explain the strengths of UV absorption lines for cosmic abundances. The covering factor of low ionization ionic species such as HI is much smaller than those of high ionization species (up to 80%). But they did not make any specific statement about the global covering factor of the gas. This model is consistent with the ROSAT data for this source. However, if we want to extend this model to other BAL QSOs, such as PG 1001+043, we have to require that the total covering of the absorber is close to unity in order to explain their weakness in the ROSAT band as we proposed for PG 1001+054.

6. CONCLUSION

We show that the opacity of soft X-rays at energies between 0.2-0.35 keV is dominated by L-shell photo-electric absorption of oxygen and neon in the X-ray absorber of BAL QSOs. A stringent limit on the ionization parameter can be set by requiring presence of sufficient column densities for the ions responsible for the absorption in the soft X-ray band, namely, OVI, NeVII and NeVIII. For typical equivalent hydrogen column density of $10^{23.5} \text{ cm}^{-2}$, the ionization parameter is required: $U_x < (0.2 - 0.3)$, or $U_H < 10$ for the typical spectral energy distribution of radio-quiet QSOs. We find that the X-ray absorber has to have very large column densities in OVI, NeVII and NeVIII of the order of $10^{17-18} \text{ cm}^{-2}$ in order to have sufficient opacity in the soft X-ray band. Since these column densities are derived from the observed optical depth in the soft X-ray band, they do not strongly depend on the specific ionization continuum and the detail metal abundance. For reasonable ionizing continuum, it will also produce large column densities in CIV, NV and HI of order a few 10^{16} cm^{-2} .

These results are compared with the observed X-ray and UV spectra for several BAL QSOs with available soft X-ray data. In PG 1411+442, a uniformly covering absorption model can explain the observed UV and X-ray absorption.

However, in PG 1001+054, the UV absorption lines predicted from the X-ray absorption are much stronger than the observed ones, if the X-ray absorption material uniformly covers the UV continuum source. The discrepancy can be solved by a locally partial covering model in which the thick flow or clouds at a specific velocity covers only a certain fraction of the line sight to the continuum, but the total covering factor of all clouds or the flow is close to 1. As the covering factor of the absorber at any specific projected velocity is strongly viewing angle dependent, this model has enough flexibility to produce the different BAL behaviors. This model might also apply to those BAL QSOs for which ROSAT yielded stringent upper limits on the X-ray flux but where the UV continuum is only partially absorbed.

Our work shows that, assuming the X-ray and UV absorbers being the same, self-consistent absorption models can be constructed to explain the X-ray and UV observations of the BAL QSOs treated herein; we thus suggest it as a promising case in BAL objects. However, future observations with a better sample and better quality data are need to draw firm conclusion on this, considering following caveats of the analysis presented in this paper: (1) The QSOs herein, and especially PG 1411+442, may not be representative of BAL QSOs. (2) the assumption that the intrinsic SEDs are like those observed in other non-BALQSOs used in deriving the observed CIV and OVI column density,

While the absorber can contribute significantly to the extremely highly ionized emission lines, such as O VI 1032/1037Å and Ne VIII 770/780Å if it covers a substantial fraction of solid angle and if the density is higher than 10^8 cm^{-3} , it has very little impact on the medium and low ionization UV lines such as NV, CIV and Ly α . The profiles of NeVIII and OVI lines may be indicators for the kinematics of the X-ray absorber in QSOs. The observed Ne VIII line profiles in QSOs suggests that the velocity of the gas projected onto our line of sight is similar to that seen in the outflows of the UV BALs.

We thank S. Komossa for critical reading of this manuscript and an anonymous referee for helpful comments. TW acknowledges the financial support from Chinese NSF (19925313) and from the Chinese Science and Technology Ministry.

REFERENCES

Arav N., Li Z., & Begelman M. 1994, ApJ, 432, 62
 Arav N., Korista K.T., de Kool, M., Junkkarinen V. T., Begelman M.C., 1999, ApJ, 516, 27
 Brandt W.N., Laor A., Wills B.J., 2000, ApJ, in press.
 Brinkmann W., Wang T., Matsuoka M., Yuan W., 1999, A&A, 345, 43
 Cohen,M.H., Ogle P.M., Tran H.D., Vermeulen R.C., Miller J.S., Goodrich R.W., Martel A.R. 1995, ApJ, L77
 Dumont, A., Abrassart A., Collin S., 2000, A&A, in press (astro-ph/0003220)
 Ferland, G.J., 1999, Hazy, a brief introduction to Cloudy 90.
 Gallagher S.C., Brandt W.N., Sambruna R.M., & Mathur S., 1999, ApJ, 519, 549
 Green P.J., Schartel N., Anderson S.F., Hewett P.C., Foltz C.B., Brinkmann W., Fink H., Truemper J. & Morgan B. 1995, ApJ, 450, 51
 Green P.J., & Mathur S. 1996, ApJ, 450, 51
 Hamann F. 1998, ApJ, 500, 798
 Hamann F., Korista, K.T., & Morris, S.L. 1993, ApJ, 415, 541
 Korista K.T., Ferland G.J., & Baldwin J. 1997, ApJ, 487, 555
 Korista T., & Arav N., 1997, in ASP. Conf. Ser. 128, Mass Ejection from AGN, ed. N. Arav I. Shlosman & R.J. Weymann (San Francisco:ASP), 201
 Korista K.T., Weymann R.J., Morris S.L., et al., ApJ, 401, 529
 Laor A., Fiore F., Elvis M., Wilkes B.J., McDowell J.C., 1997, ApJ, 477, 93
 Mathews, W.G., & Ferland, G.J., 1987, ApJ, 323, 456
 Mathur, S., et al., 2000, ApJL, submitted
 Murray N., Chiang J., Grossman S.A., & Voit G.M., 1995, ApJ, 451, 498
 Netzer, H. 1990 in Active Galactic Nuclei, eds. Balndford, R.D., Netzer, H., & Woltjer L., (Springer-Verlag: Berlin).
 Netzer, H. 1996, ApJ, 473, 781
 Neugebauer G., Green R.F., Matthews, Schmidt M., Soifer B.T., Bennett J., 1987, ApJS, 63, 615
 Schmidt G.D., Hines D., 1999, ApJ, 512, 125
 Telfer R.C., Kriss A., Zheng W., Davidsen A.F., Green R.F., 1998, ApJ, 509, 132
 Turner, T. J. 1999, ApJ, 511, 142
 Wang T., Brinkmann W., Bergeron J., 1996, A&A, 309, 81

Wang T.G., Lu Y.J., & Zhou Y.Y., 1998, ApJ, 493, 1
Wang T.G., Wang J.X., Brinkmann W., & Matsuoka M., 1999, ApJ,
519, L31

Weymann R.J., Morris S.L., Foltz C.B., & Hewett P.C., 1991, ApJ,
373, 23
Zheng W., Kriss G.A., Telfer R.C., Grimes J.P. & Davidsen A.F.,
1998, ApJ, 492, 855

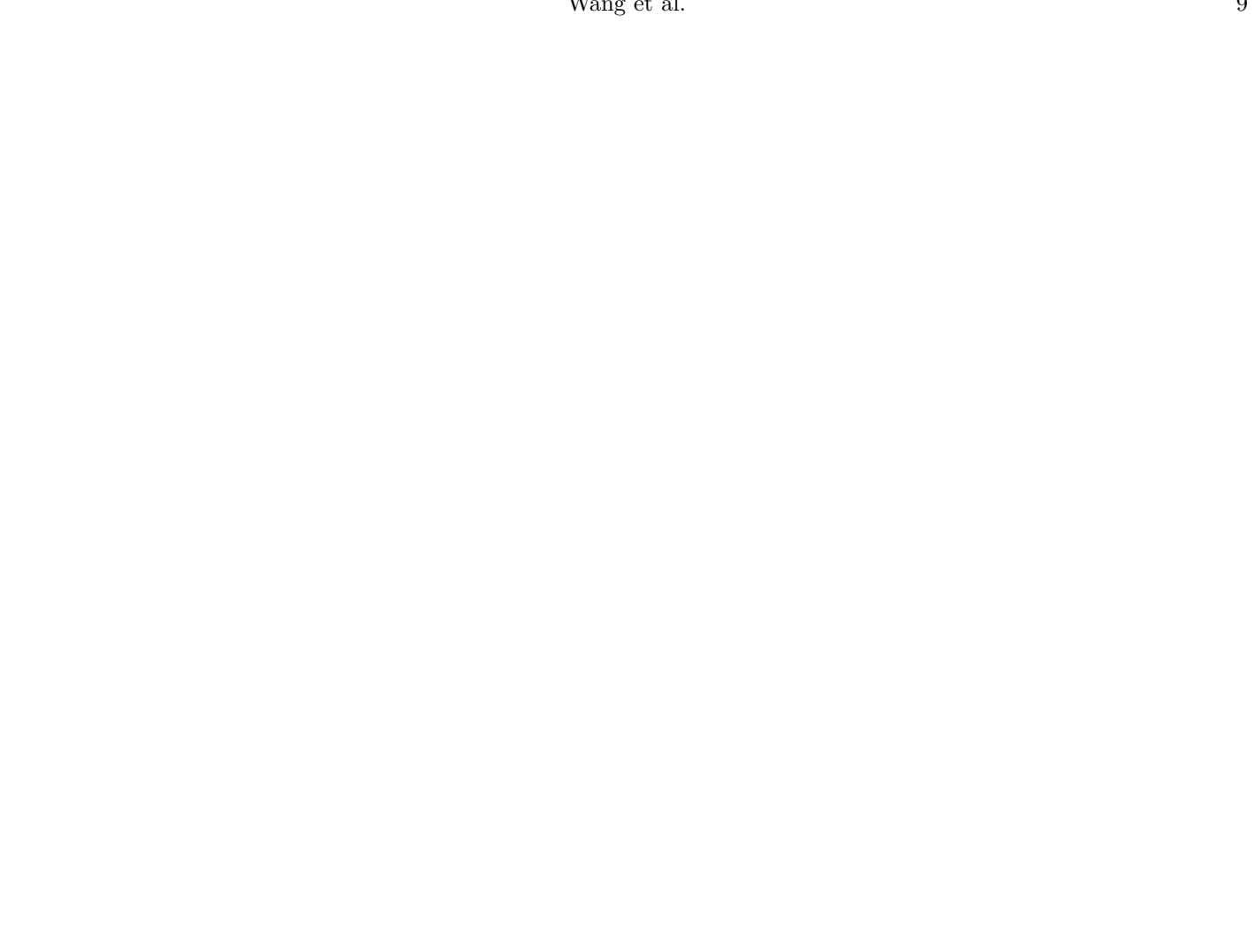


FIG. 1.— The Spectral Energy Distribution of three BAL QSOs detected with ROSAT. The optical and UV spectra have been corrected for Galactic reddening. The dashed line shows the average SED for radio-quiet quasars from a composite of HST and the low redshift ROSAT PG quasar sample (Zheng et al. 1998). Spectra have been shifted vertically arbitrarily for clarity.

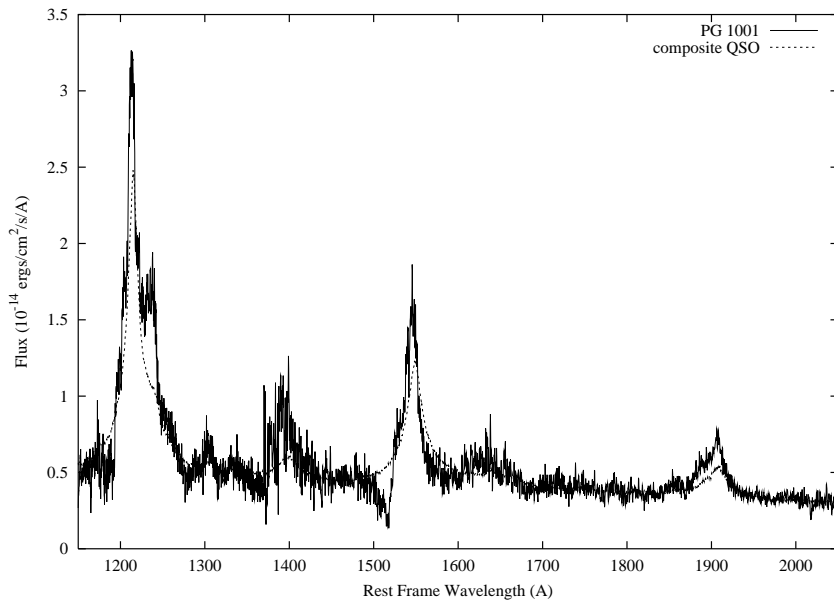


FIG. 2.— A comparison of the UV spectrum of PG 1001+054 (solid line) with the HST composite QSO spectrum (dotted line) showing strong HeII $\lambda 1640$ and other high ionization lines.

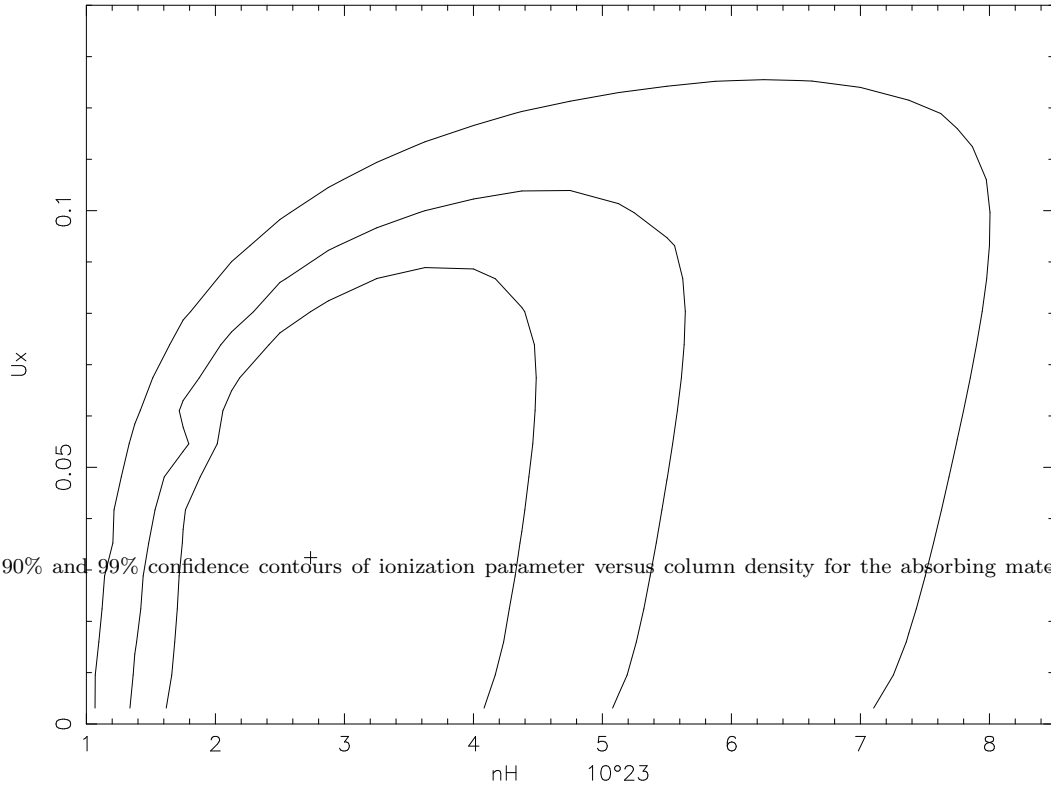


FIG. 3.— The 68%, 90% and 99% confidence contours of ionization parameter versus column density for the absorbing material in PG 1411+442.

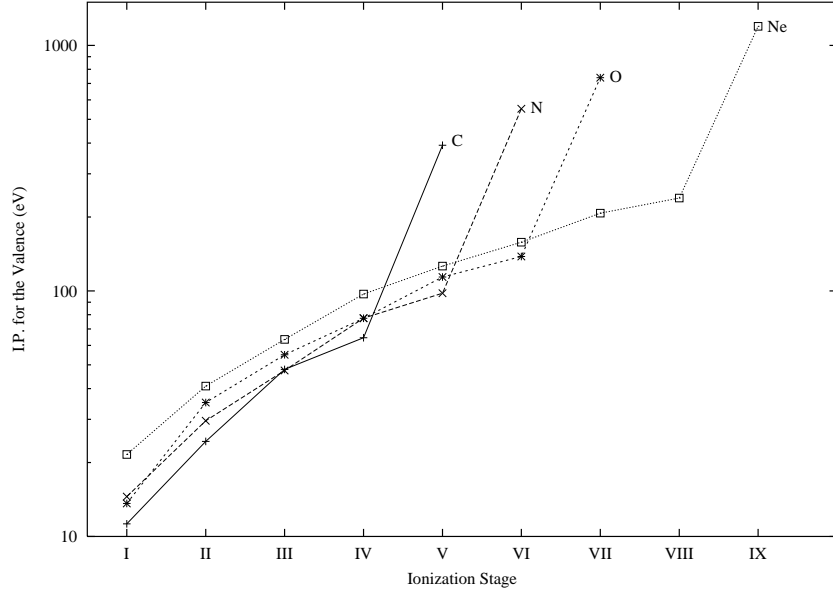


FIG. 4.— Plot of ionization potential versus ionization stage for valence electrons for elements C, N, O and Ne. Notice that the ionizing potentials for K-shell electrons are larger than 0.39 keV for these elements.

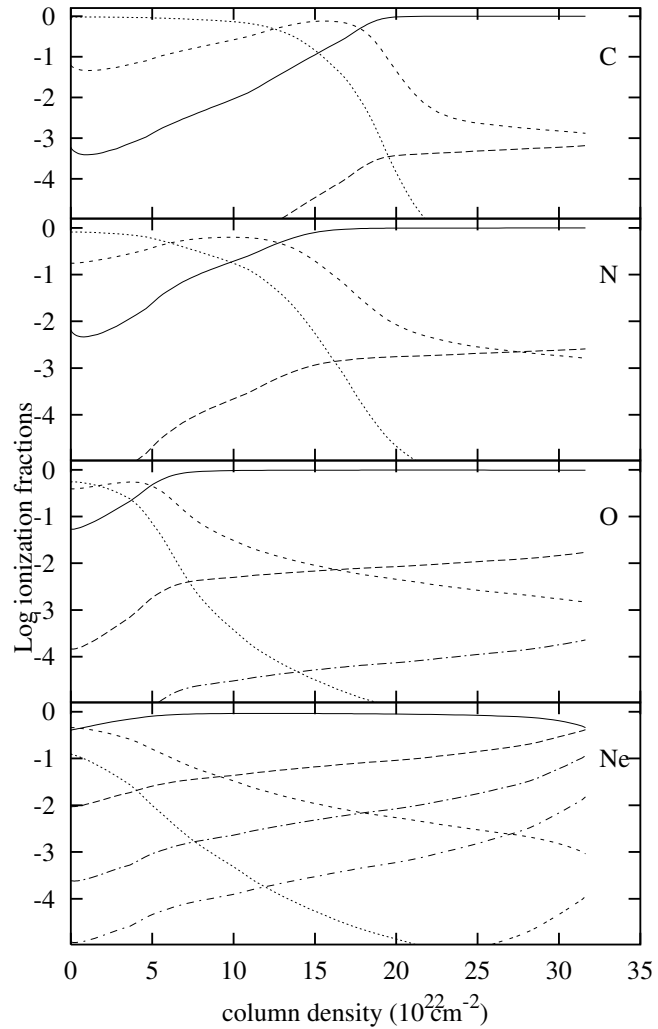


FIG. 5.— The ionization structure of the elements C, N, O, and Ne for an ionization parameter 10 and a column density $10^{23.5} \text{ cm}^{-2}$. The curves show the logarithm of fraction of ion species, starting with a fully stripped ion on the left, with decreasing ionization stages toward the right.

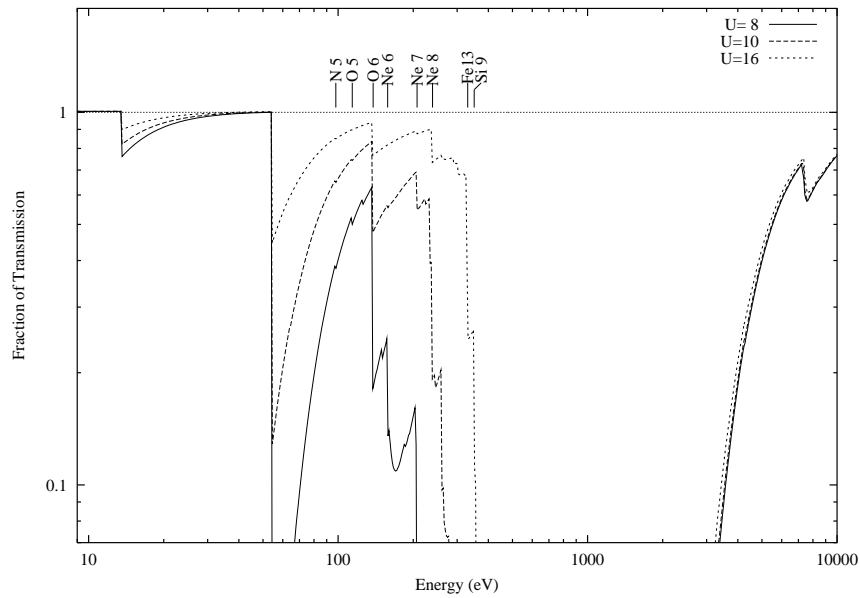


FIG. 6.— The transmission rate of the ionization continuum in the 10 eV to 10 keV energy range for $U_H = 8, 10$, and 16 corrected for Thomson scattering.

